2011 IEEE International Conference on Robotics and Automation
Shanghai International Conference Center
May 9-13, 2011, Shanghai, China

High-Accuracy GPS and GLONASS Positioning by Multipath Mitigation using Omnidirectional Infrared Camera

Taro Suzuki, Mitsunori Kitamura, Yoshiharu Amano and Takumi Hashizume

***Abstract*—This paper describes a precision positioning technique that can be applied to vehicles or mobile robots in urban or leafy environments. Currently, the availability of satellite positioning is anticipated to improve because of the presence of various positioning satellites such as GPS of the U.S., GLONASS of Russia and GALILEO of Europe. However, because of the serious impact of multipath on their positioning accuracy in urban or leafy areas, such improvements in the availability of satellite positioning do not necessarily also facilitate high precision positioning. Our proposed technique mitigates GPS and GLONASS multipath by means of an omnidirectional infrared (IR) camera that can eliminate the need for invisible satellites by using IR images. With an IR camera, the sky appears distinctively dark. This facilitates the detection of the borderline between the sky and the surrounding buildings, which are captured in white, because of the difference in the atmospheric transmittance rates between visible light and IR rays. The proposed technique can automatically and robustly mitigate GPS and GLONASS multipath by excluding the invisible satellites. Positioning evaluation was carried out only with visible satellites that have less multipath errors and without using invisible satellites. The evaluation results confirm the effectiveness of the proposed technique and the feasibility of its highly accurate positioning.**

I. Introduction

Currently, the applications of a global navigation satellite system (GNSS) are rapidly gaining popularity. With the planned GPS modernization programs of the U.S., GLONASS of Russia, GALILEO of Europe, and the launch of quasi-zenith satellites by Japan, an improvement in the availability of satellite positioning is anticipated [1]. Indeed, 30 GPS satellites and 17 GLONASS satellites have become available in February 2010, and they are expected to increase the application of mobile systems in outdoor environments, such as unmanned construction site systems with autonomous construction machinery and automatic vehicle navigation.

However, because of the serious impact of multipath on the positioning accuracy in urban or leafy areas, such improvements in the availability of satellite positioning do not necessarily also facilitate high precision positioning [2][3]. In addition, high precision positioning using GNSS in urban or leafy areas is desired in the field of intelligent transportation systems (ITS) [4][5]. Mobile mapping systems [4], for example, require continuous, accurate self-positioning even near high-rise buildings, which are particularly responsible for generating multipath error. It is therefore essential to establish a positioning technique that will sort out the available satellites and use only those with the least multipath errors [6]–[13].

On the other hand, simple techniques such as the installation of antennas away from buildings and the use of choke ring antennas are known to contribute toward multipath mitigation; however, these techniques are either impractical or have very limited applications. Various correlator and receiver autonomous integrity monitoring (RAIM) [6] techniques can also be used for multipath mitigation; these techniques are highly practical and popular. The narrow-correlator technique [7] proposed in the early 1990s can eliminate multipath errors better than the former methods. The early-late slope technique [8] and the strobe-correlator technique [9] were also developed in the 1990s. Currently, the use of multipath-estimating delay-locked loops (MEDLLs) [10] is widespread, and a vision correlator technique [11] has also been developed. RAIM provides an alert by checking between the position solutions obtained from satellite signals.

Various correlator techniques can also be employed. However, when a direct signal cannot be received by an antenna, these techniques do not provide satisfactory results because they presume that it is the antenna that principally receives direct signals. Fig. 1 illustrates this principle. There are many situations in urban areas in which there is a large multipath error from invisible satellites, and it is difficult to determine and mitigate such errors from the signals alone.

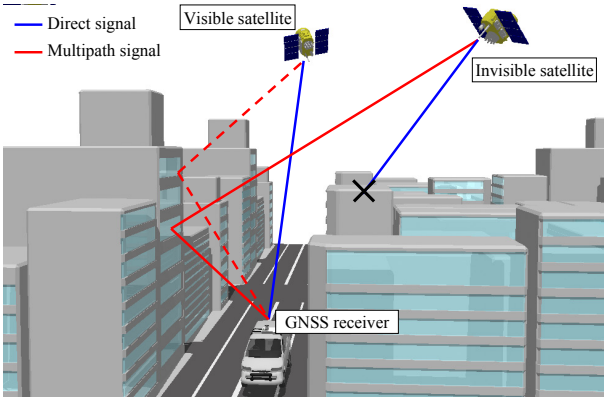

Fig. 1 Multipath signals from visible and invisible satellites.

Manuscript received February 28, 2010. This work was supported in part by the Research Fellowships of the Japan Society for the Promotion of Science for Young Scientists.

Author T. S. and M. K. are with the Graduate School of Science and Engineering, Waseda University, Tokyo, Japan (phone: +81-3-3203-4515; fax: +81-3-3203-3231; e-mail: taro@power.mech.waseda.ac.jp).

Y. A. and T. H. are with the Advanced Research Institute for Science and Engineering, Waseda University, Tokyo, Japan

Therefore, multipath mitigation techniques to distinguish invisible satellites from visible satellites have now come to the forefront. A multipath simulation method that uses 3D geographic information systems (GIS) [12], which simulate multipath by pre-measuring building height information, has been proposed. An evaluation tool to predict the availability of a satellite's constellation service along a given terrestrial trajectory by means of a visible light fish-eye optic system [13] has also been proposed.

In these studies, it is possible to improve the positioning accuracy in order to exclude invisible satellites in the limited situation in which signals are being received from many satellites. The number of satellites used for positioning is decreased by excluding the invisible satellites. This increases the dilution of precision (DOP), which in turn reduces the positioning accuracy. In addition, these methods are not practical because they are difficult to automate and present problems in robustness analysis.

In this paper, we describe a precision positioning technique that can be applied to vehicles or mobile robots in urban or leafy areas, and we propose a technique to realize multipath mitigation that uses an omnidirectional IR camera to exclude invisible satellites. We use a combination of GPS and GLONASS signals to increase the input from visible satellites. This technique employs an omnidirectional IR camera and a satellite orbit simulator to automatically determine the geometrical relationship between the satellites and the obstructions, as seen from the vehicle; this enables operation with only satellites that have small multipath errors by excluding invisible satellites from the positioning computation. In addition, the proposed technique can mitigate GPS and GLONASS multipath even if a direct signal cannot be received, because it can recognize the surrounding environment by using an omnidirectional IR camera.

The rest of the paper is organized as follows. Section 2 provides an outline of the proposed technique. Section 3 describes the IR omnidirectional camera and obstacle detection. Section 4 analyzes the multipath error from visible and invisible satellites. Finally, Section 5 evaluates the positioning precision achieved by our proposed technique.

II. Outline of the Proposed Technique

In order to exclude the radio waves emitted from invisible satellites, the satellites' positions, the vehicle position and attitude, and the physical relationship between the satellites and the obstructions blocking the radio waves from the satellites must be identified at all times to determine the visibility of the satellites. The technique proposed herein involves the exclusion of invisible satellites by observing the satellite positions using a satellite orbit simulator, the vehicle heading angle with an angular displacement sensor such as a gyroscope, and the obstruction positions using an omnidirectional IR camera. The specific algorithm employed in this technique is shown in Fig. 2. First, to obtain the elevation and the azimuth angles of the satellite as seen from the vehicle, the position of the satellite is obtained by the GPS and GLONASS receiver. The satellite position is converted into the elevation and the azimuth angles by using the approximate position of the vehicle as obtained from the GPS and GLONASS receiver and the angular displacement sensor. Here, even if the approximate position of the vehicle is significantly shifted from the actual position, the shift is small in comparison to the distance between the satellite and the vehicle; thus, the elevation and the azimuth angles are hardly affected and remain sufficient for accurate computation, even for GPS and GLONASS point positioning. The system then proceeds with a simple segmentation of the omnidirectional IR camera image to obtain knowledge of the obstruction positions as seen from the vehicle. Next, the omnidirectional IR camera image is set on the plane of the elevation and azimuth angles. Then, the satellite positions are plotted on the image with the obstructions in order to determine the visibility of each satellite in the image of satellites and obstructions superimposed on one another. Finally, positioning is carried out using only the visible satellites that have small multipath errors and without using the invisible satellites.

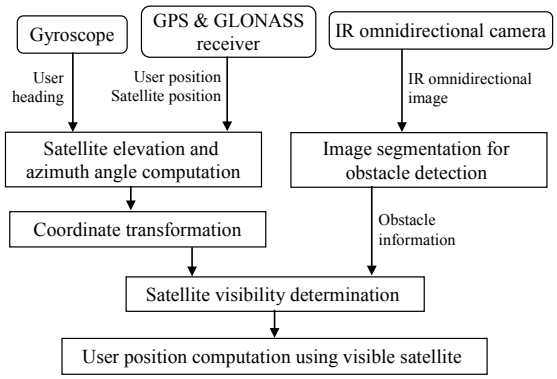

Fig. 2 Multipath mitigation algorithm using omnidirectional IR camera.

III. Visible Satellites Selection using IR Image

A. Developed Omnidirectional Far-Infrared Camera

The omnidirectional far-IR camera developed in this study for the detection of obstacles is shown in Fig. 3. This camera can generate IR images with an elevation of 20°–70° for the entire surrounding area over 360° [14]; it is capable of taking clear images of buildings or foliages even at night. A two-mirror optic system is adopted because in the case of far-infrared rays, it is easier to design than a wide angle lens such as a fish-eye lens. Fig. 4 shows images taken simultaneously in the same place by a visible-light fisheye camera and an omnidirectional IR camera during both daytime and nighttime. With the IR camera, the sky is distinctively dark. This makes it easy to detect the borderline between the sky and the obstacles such as the buildings or foliages, which are captured in white, due to the difference in the atmospheric transmittance rates between visible light and far-IR rays [15]. Furthermore, halation of the charge coupled device (CCD) image sensor caused by sunlight and street

lights is observed in the fisheye camera image in Fig. 4, while this is not observed in the omnidirectional IR camera images. Therefore, using an omnidirectional IR camera enables robust determination of the borderline between an object and the sky in the presence of outdoor lights and other disturbances; thus, it is possible to reliably identify the borderline even in the case of image processing using simple binarization.

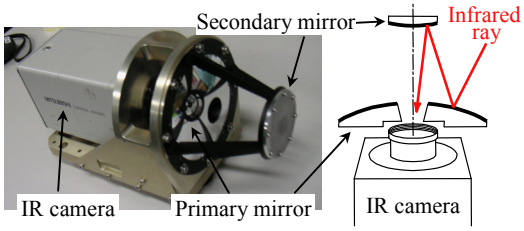

Fig. 3 Omnidirectional IR camera and optic system.

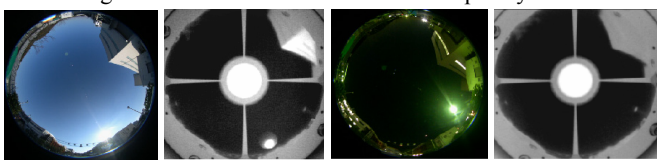

(a) Fish-eye (b) Omnidirectional IR (c) Fish-eye (d) Omnidirectional IR

Fig. 4 Comparison of images from color fisheye camera and omnidirectional IR camera. (a) and (b) are during the daytime. (c) and (d) are during the nighttime.

B. Obstacle Detection from Omnidirectional Images

To detect obstacles from omnidirectional IR images, image binarization is carried out in order to divide the surrounding environment into two categories: the sky and objects such as buildings. There is a difference between the atmospheric transmittance rates of visible light and far-IR rays. Far-IR rays, however, are affected by the cloud cover at the time of image acquisition. Fig. 5 shows two IR images obtained at the same place, one on a clear day and one on a cloudy day. The image on the cloudy day captured the clouds in a gray tone. To separate the clouds from the obstacles, a variable threshold must be used for image binarization. The image intensity histograms for a clear day and a cloudy day are shown in Fig. 5. Each histogram has three peaks, and it is considered that each peak corresponds to the image of the sky including clouds, obstacles, and mirror and pillar of the camera, respectively. It can be concluded that the intensity between peak 1 and peak 2 can be used as the threshold to divide an IR image into the sky and obstacles.

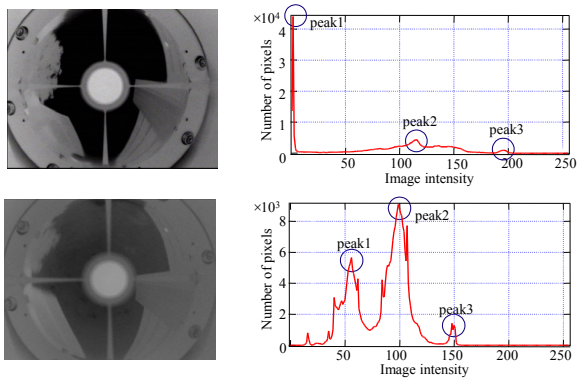

Fig. 5 Comparison of a clear day (top) and a cloudy day (bottom).

C. Selection of Visible Satellites

In this process, visible satellites are selected as seen from the user position by using the binarized IR omnidirectional image. The satellite position from the GPS and GLONASS receiver is converted into the elevation and the azimuth angles of the satellite by using the GPS and GLONASS point positioning, which uses all the satellites and the angular displacement sensor. After the computation of the elevation and the azimuth angles, the omnidirectional IR camera image is set on the virtual image plane of the elevation and azimuth angles. In this computation, the intrinsic parameters of the camera are necessary in order to determine the virtual image plane, and these parameters are assumed to have been calibrated in advance. Fig. 6(a) shows the relationship between the omnidirectional image and the satellite position. Next, the satellite positions are plotted to determine the visibility of each satellite from the overlapping of the satellites and the obstructions. Fig. 6(b) shows the satellite position superimposed upon the binarized IR image. The visibility of a satellite is easily determined by checking the value of the pixels in the binarized image of the satellite position. This process is carried out completely automatically in synchronization with the acquisition of GPS and GLONASS data.

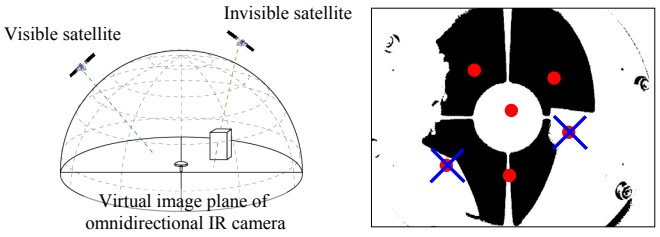

(a) Virtual camera image plane (b) Selection of visible satellites

Fig. 6 Determination of satellite visibility using IR omnidirectional camera.

IV. Multipass Error Assessment

In order to confirm the effectiveness of the exclusion of invisible satellites to obtain accurate positioning, a static positioning test was performed. We calculated and analyzed the multipath errors of visible and invisible satellites at a predetermined position to evaluate the influence of multipath caused by obstacles. The computation was performed with code multipath errors. First, we describe the calculation of multipath error from a pseudorange of the GPS and GLONASS data. Next, we assess the multipath error of invisible satellites as computed by an IR omnidirectional camera.

A. Algorithm for Multipath Errors

Here, an algorithm to calculate the multipath error $\varepsilon_u^{(k)}$ of a satellite k is provided. The code pseudorange for satellite k can be expressed by Eq. (1) as follows:

$$\rho_u^{(k)} = r_u^{(k)} + I + T + c(\delta t_u - \delta t_s^{(k)}) + \varepsilon_u^{(k)} \quad (1)$$

where $\rho_u^{(k)}$ denotes the pseudorange of the user station; $r_u^{(k)}$, the satellite-to-receiver distance; I, the ionospheric delay; T, the tropospheric delay; c, the velocity of light; δt_u, the clock bias of the receiver; and $\delta t_s^{(k)}$, the clock bias of the satellite k. In this study, we presume that, in comparison with the multipath errors, the noise errors of the receiver are small enough to be ignored.

When a differential correction at the reference station with a short baseline is applied to Eq. (1), Eq. (2) is obtained.

$$\rho_{ur}^{(k)} = r_{ur}^{(k)} + c\delta t_{ur} + \varepsilon_{ur}^{(k)} \tag{2}$$

where $\rho_{ur}^{(k)}$ denote $\rho_r^{(k)} - \rho_u^{(k)}$; $r_{ur}^{(k)}$, $r_r^{(k)} - r_u^{(k)}$; δt_{ur}, $\delta t_r - \delta t_u$; and $\varepsilon_{ur}^{(k)}$, $\varepsilon_r^{(k)} - \varepsilon_u^{(k)}$.

Further, taking the double difference with a differentially corrected reference satellite l, Eq. (2) is expressed as Eq. (3).

$$\rho_{ur}^{(kl)} = r_{ur}^{(kl)} + \varepsilon_{ur}^{(kl)} \tag{3}$$

With regard to Eq. (3), the static positioning in this test was carried out at a known location, and the value $r_{ur}^{(kl)}$ could be calculated accurately; thus, it is possible to calculate $\varepsilon_{ur}^{(kl)}$. However, the multipath error $\varepsilon_{ur}^{(kl)}$ includes not only the multipath errors of the satellite but also the multipath errors of the reference station and reference satellite l. Now, because the reference station is in an open location where multipath hardly occurs, we presume the error to be minor. In addition, with regard to the reference station, we can presume that the multipath errors will be minor by selecting a satellite with a high elevation angle that is not blocked by the surrounding buildings. With the above considerations, we compute the multipath error $\varepsilon_u^{(k)}$ of satellite k.

$$\varepsilon_u^{(k)} = \left| \rho_{ur}^{(kl)} - r_{ur}^{(kl)} \right| \tag{4}$$

B. *Pseudorange Errors of Invisible Satellites*

Multipath error evaluation tests were performed on October 20, 2009 at a predetermined position at Waseda University in Tokyo, Japan. GPS and GLONASS data were obtained at a rate of 1 Hz in static observations. The surroundings of the observation point consisted of scattered tall buildings, making it an environment susceptible to satellite masking. The receiver was a DELTA-G2T (JAVAD Inc.) with the elevation angle mask set at 10°. The reference station was installed at a nearby observation point (baseline length of approximately 30 m) in an open location. Multipath error computation was carried out by post-processing with code-DGNSS positioning represented by Eqs. (1)–(4).

First, the multipath error of the visible satellites was computed. Fig. 7(a) shows the IR omnidirectional image and the trajectory of the PRN5 satellite from 133178 to 136778 GPS seconds. This PRN5 satellite was determined to be a visible satellite by the proposed method, a result which is indicated in Fig. 7(a). A graph that shows the signal strength (carrier-to-noise (C/N) ratio) and the multipath errors obtained by Eq. (4) is presented in Fig. 7(b). As can be seen, PRN5 has short-delay multipath errors (approximately 3 m RMS); however, this does not present a serious problem for positioning.

Next, the multipath errors of PRN11, which is in the same time period from 197978 to 201578 GPS seconds, was determined to be an invisible satellite by the proposed technique at approximately the same angle of elevation as that of PRN5, as shown in Fig. 8. During this time period, the receiver continually received radio waves from the invisible satellite PRN11. In Figs. 7(b) and 8(b), it can be observed that the invisible satellite PRN11 has extremely large multipath errors (approximately 60 m) as compared to satellite PRN5. In other words, invisible satellites have a large multipath error as compared to visible satellites in this case, and it can be presumed that the positioning error will be increased using this invisible satellite PRN11.

Next, a multipath mitigation technique that uses the correlation between the signal strength and the short-delay multipath errors is introduced [16]. In Fig. 7(b), PRN5 with short-delay multipath errors shows a correlation between a decrease in signal strength and an increase in multipath errors; however, in Fig. 8(b), PRN11 with long-delay multipath errors does not exhibit any notable correlation between its signal strength and multipath errors, which makes it difficult to detect any malfunctioning due to signal strength. Positioning computation was therefore possible with the exclusion of PRN11, which was determined to be an invisible satellite by the proposed technique. On the basis of the above observations, it can be stated that signals from invisible satellites include large multipath errors, and the positioning accuracy can be expected to improve by excluding the invisible satellites using the proposed technique.

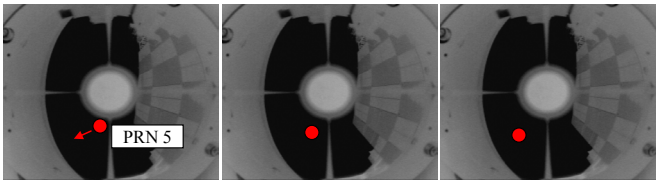

(a) Position of visible satellite on IR image

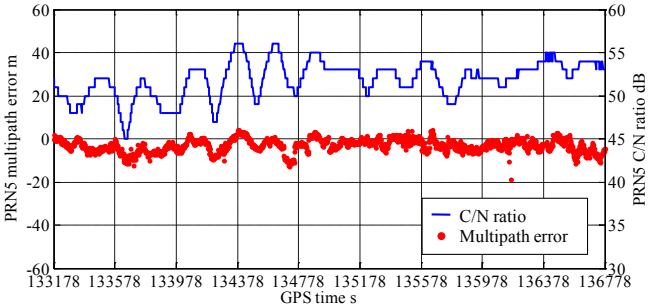

(b) C/N ratio and multipath error

Fig. 7 C/N ratio and multipath error (visible satellite).

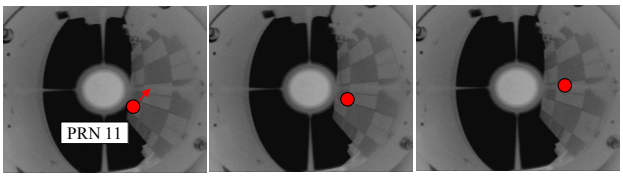

(a) Position of invisible satellite on IR image

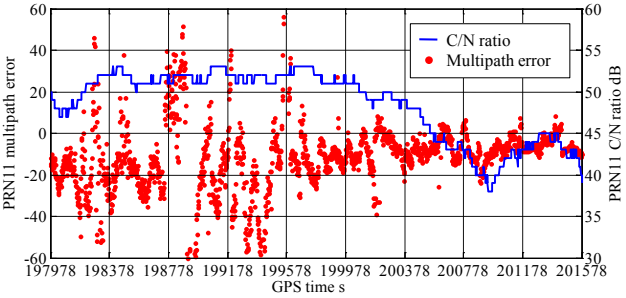

(b) C/N ratio and multipath error

Fig. 8 C/N ratio and multipath error (invisible satellite).

V. Evaluation of Positioning Precision

A. Experimental Environments and Methods

In order to confirm the effectiveness of the proposed technique, a kinematic positioning test was performed at Waseda University in Tokyo, Japan on October 20, 2009. The mobile robot used in the test is shown in Fig. 9. The GPS and GLONASS receiver with a 10° elevation angle mask, antenna, and IR omnidirectional camera were installed together. The experimental environment and the planned path are shown in Fig. 10. To be able to compare the positioning accuracy, we set up ground control points (GCPs), which are predetermined high-accuracy positions, and a reference path connecting the GCPs in the actual environment shown in Fig 10(a) and (b). The GPS and GLONASS data were obtained at a rate of 1 Hz. The mobile robot traveled approximately 150 m on the reference path with its speed manually controlled at 4 km/h. Evaluation was carried out by post-processing with code-DGNSS positioning.

B. Experimental Results

The number of satellites used for positioning by the proposed technique is shown in Fig. 11. The number of satellites is compared between using only GPS in Fig. 11(a) and combining GPS and GLONASS in Fig. 11(b). In Fig. 11(a), there are many instances where the numbers of satellites is less than 4 because of the exclusion of invisible satellites by the buildings and trees around the observation point. In such cases, it may be presumed that the multipath error can be mitigated even though the positioning accuracy is decreased because of the reduction in the number of satellites. Compared to Fig. 11(a), which uses both GPS and GLONASS, Fig. 11(b) shows an increase in the number of satellites at all times. The average number of satellites using only GPS is 6.5 before satellite exclusion and 4.3 after satellite exclusion. Using both GPS and GLONASS, the average number of satellites is 9.3 before satellite exclusion and 6.8 after satellite exclusion.

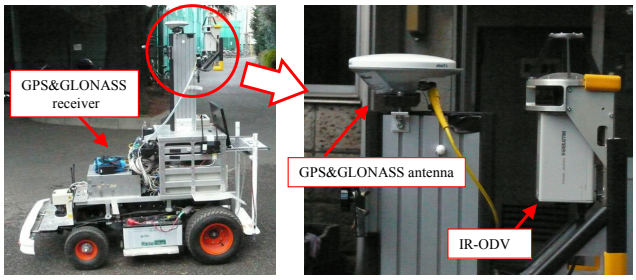

Fig. 9 Experimental vehicle installed with omnidirectional IR camera and GNSS receiver.

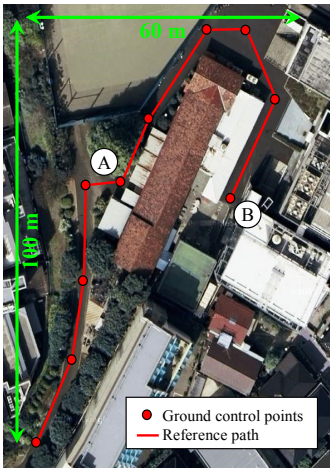

(a) Experimental environment

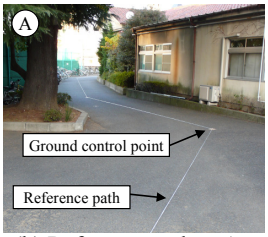

(b) Reference path at A

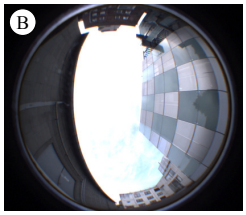

(c) Fish-eye image at B

Fig. 10 Test environment for dynamic evaluation.

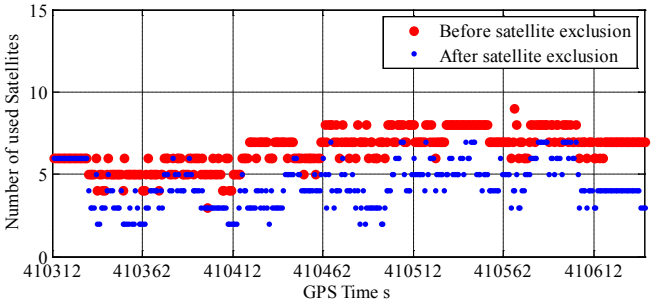

(a) Number of satellites using GPS

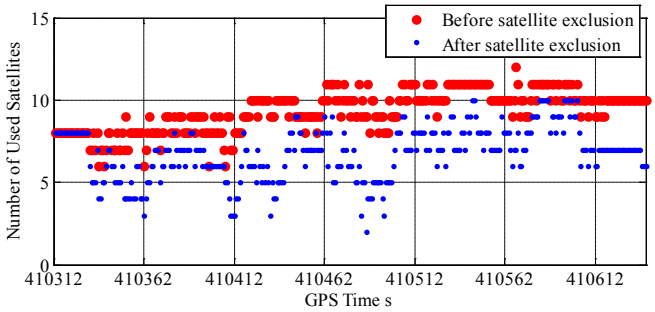

(b) Number of satellites using GPS and GLONASS

Fig. 11 Comparison between the number of satellites when only GPS is used and when both GPS and GLONASS are used.

Plotting of the satellite geometry on the omnidirectional IR camera images at 410362 and 410412 GPS seconds is shown in Fig. 12. Some signals from GPS and GLONASS satellites

were received; however, they were from invisible satellites. In this case, by combining GPS and GLONASS, it becomes possible to retain satellite information for positioning.

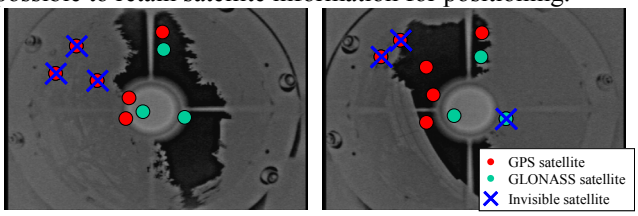

Fig. 12 Visible satellites in dynamic evaluation test.

Fig. 13(a) shows a comparison of the positioning accuracy (distance error) obtained before and after the exclusion of invisible satellites, which were determined by the proposed method using only GPS. The positioning error is increased to exclude the invisible satellites, which have a large multipath. This can be explained as being the result of the decrease in the number of satellites, which affects the positioning accuracy, as shown in Fig. 11(a). In comparison with Fig. 13(a), Fig. 13(b) shows that the positioning accuracy obtained by using both GPS and GLONASS is increased using the proposed technique at almost all the time. The two-dimensional distance root mean square (2DRMS) errors of the GPS and the GPS and GLONASS solutions before and after the exclusion of invisible satellites were calculated. As shown in Fig. 13(a), by excluding invisible satellites, the error is increased from 1.56 m to 3.89 m. Using both GPS and GLONASS for positioning, the error is decreased from 1.17 to 0.72 m before and after exclusion. From these results, it can be stated that the proposed technique is effective in kinematic positioning and offers increased positioning accuracy in urban environments, which cause a large multipath error in GNSS signals.

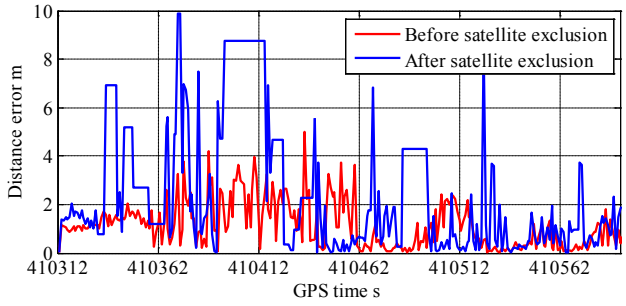

(a) Positioning accuracy using GPS

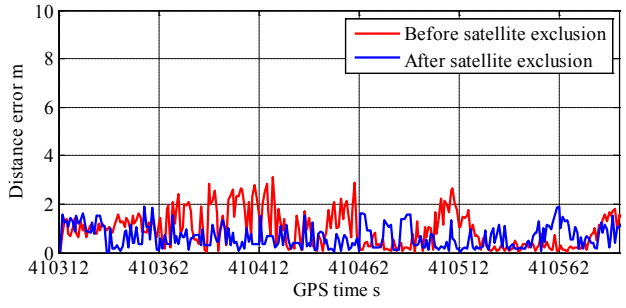

(b) Positioning accuracy using GPS and GLONASS

Fig. 13 Comparison between distance errors in the two approaches.

VI. Conclusions

Against the background of an increasing number of satellites, it is essential to establish a technique that can select satellites with small multipath errors in order to achieve high precision positioning at all times. In this paper, we have therefore proposed a technique with which the obstruction of satellite signals can be determined using an omnidirectional IR camera, allowing improvement in the accuracy of mobile positioning in urban or leafy areas by excluding the invisible satellites.

Using the proposed technique, kinematic evaluations were carried out in which invisible satellites were excluded through observations made using an omnidirectional IR camera. Signals were received even when the GPS and GLONASS satellites were blocked by buildings, and the exclusion of satellites having large errors from the positioning computation became possible. The test results confirmed the effectiveness of the proposed technique and the feasibility of high precision positioning.

References

[1] Martin Unwin, "Galileo program overview and Giove-A mission," *GPS/GNSS symposium 2006*, Tokyo.

[2] Kee Changdon, et al., "Calibration of multipath errors on GPS pseudorange measurements," *Proc. of the 7th Int. Technical Meeting of the Satellite Division of the Institute of Navigation*, pp. 353-362, 1994.

[3] Jean-Claude Bibaut, et al., "Characterization of multipath on land and sea at GPS frequencies," *Proc. of the 7th Int. Technical Meeting of the Satellite Division of the Institute of Navigation*, pp. 1155-1171, 1994.

[4] K. Ishikawa, et al., "A Mobile Mapping System for Precise Road Line Localization Using Single Camera and 3D Road Model," *Journal of Robotics and Mechatronics*, vol.19, No.2, pp.174-180, 2007.

[5] Soubielle, J., et al., "GPS positioning in a multipath environment," *IEEE Transactions on Signal Processing*, vol. 50, pp. 141-150, 2002.

[6] R. Grover Brown, "GPS RAIM: Calculation of Thresholds and Protection Radius Using Chi-Square MethodsA –Geometric Approach, *RTCA Paper* No. 491-94/SC159-584, 1994.

[7] AJ Van Dierendonck, et al., "Theory and Performance of Narrow Correlator Spacing in a GPS Receiver," *Journal of the Institute of Navigation*, Vol.39, No.3, pp.265-283, 1993.

[8] B. Townsend, et, al., "A practical approach to the reduction of pseudorange multipath errors in a L1 GPS receiver," *Proc. of ION GPS-94*, pp. 143-148, 1994.

[9] L Garin, JM Rousseau, "Enhanced Strobe Correlator Multipath Rejection for Code & Carrier," *Proc. of ION97*, 1997.

[10] Bryan R. Townsendl, D. J. Richard van Nee, "Performance Evaluation of the Multipath Estimating Delay Lock Loop," *ION National Technical Meeting*, Anaheim, California, January, 1995.

[11] Patrick C. Fenton, Jason Jones, "The Theory and Performance of NovAtel Inc.'s Vision Correlator," *ION GNSS 2005*, 2005.

[12] SUH YongCheo, et al., "Evaluation of Satellite-Based Navigation Services in Complex Urban Environments Using a Three-Dimensional GIS," *IEICE Transactions on Communications 2007*, pp1816-1825.

[13] Marais, J., et al., "Land mobile GNSS availability and multipath evaluation tool," Vehicular Technology, *IEEE Transactions on vehicular technology*, Vol. 54, Issue 5, 1697- 1704, 2005.

[14] J. Sleewaegen, F. Boon, "Mitigating Short-Delay Multipath: a Promising New Technique," *Proceedings of ION GPS 2001*, pp.204-213, 2001

[15] T. Hashizume, et al, "High Precision Range Estimation from an Omnidirectional Stereo System," *IEEE/RSJ Intelligent Robots and Systems*, pp.263-268, 2002.

[16] T. Suzuki, et al, "The Possibility of the Precise Positioning and Multipath Error Mitigation in the Real-time," *The 2004 International Symposium on GNSS/GPS*, 2004.